

Article

Advances in the Restoration of Buildings with LIDAR Technology and 3D Reconstruction: Forged and Vaults of the Refectory of Santo Domingo de Orihuela (16th Century)

Pascual Saura-Gómez *, Yolanda Spairani-Berrio , Jose Antonio Huesca-Tortosa, Silvia Spairani-Berrio and Carlos Rizo-Maestre 

Department of Architectural Constructions, University of Alicante, San Vicentede del Raspeig, 03690 Alicante, Spain; yolanda.spairani@ua.es (Y.S.-B.); ja.huesca@ua.es (J.A.H.-T.); silvia.spairani@ua.es (S.S.-B.); carlosrm@ua.es (C.R.-M.)

* Correspondence: pascual.saura@ua.es

Abstract: This research presents a new intervention methodology on arches and vaults of a Renaissance factory in the Colegio Santo Domingo de Orihuela (16th century) using 3D software LIDAR technology that verifies the execution process of the works studying the different charges states and structure behavior. This document aims to explain a working methodology in the monitoring of structural repair interventions in the architectural heritage, in the specific case of the replacement of traditional one-way timber joist frame slabs on structures of former, splay and groin arches between vaults. This involves the compilation and processing of two types of data: on the one hand, the analysis of the different load states to which the intervention is exposed in its different phases: initial, dismantling of the different layers of traditional construction and replacement by the new structural system; and, on the other hand, the graphic information provided by the photogrammetry techniques used to dimension and define the spatial position of the structural elements that have historically resolved the covering of the architectural space in this type of Renaissance solution. The different layers and demolished materials have been verified by analysing their constructive disposition, thicknesses, and dimensions of the elements that formed part of the initial construction system and their own weights. In addition, the new construction systems used in the restoration project generate a state of loads similar to the existing one. The LIDAR technology used in the research process provides graphic data of the spatial position of the arches and vaults studied in the different states of the construction intervention. The point clouds obtained are analysed by taking as reference fixed points (considered unalterable and infinitely rigid) of the refectory and the coordinates of the initial and final states are compared. The results show minimal variations between the two positions, which justifies the goodness of the construction methods used and the structural safety obtained in the complex. This methodology applied to arches and vaults in heritage architecture guarantees the control and recording of the movements produced in the process.

Keywords: TLS; 3D photogrammetry; cultural heritage; restoration methodology; vaults restoration; LIDAR; BIM



Citation: Saura-Gómez, P.; Spairani-Berrio, Y.; Huesca-Tortosa, J.A.; Spairani-Berrio, S.; Rizo-Maestre, C. Advances in the Restoration of Buildings with LIDAR Technology and 3D Reconstruction: Forged and Vaults of the Refectory of Santo Domingo de Orihuela (16th Century). *Appl. Sci.* **2021**, *11*, 8541. <https://doi.org/10.3390/app11188541>

Academic Editors: Massimo Coli and Yoshi Iwasaki

Received: 3 August 2021

Accepted: 31 August 2021

Published: 14 September 2021

Publisher's Note: MDPI stays neutral with regard to jurisdictional claims in published maps and institutional affiliations.



Copyright: © 2021 by the authors. Licensee MDPI, Basel, Switzerland. This article is an open access article distributed under the terms and conditions of the Creative Commons Attribution (CC BY) license (<https://creativecommons.org/licenses/by/4.0/>).

1. Introduction

The origins of the Colegio Santo Domingo de Orihuela date back to the Dominican Friars who had established themselves on the outskirts of the city and who promoted the foundation of a convent according to the papal dispensation of Pope Julius II in 1512 and royal decrees of King Ferdinand the Catholic, which were later ratified in 1528 by King Charles I. From 1546 onwards, the Bishop of Lérida, Don Fernando de Loazes, decided to build a College for the training of religious and lay people, according to the Order's act celebrated in Rome "*acceptamost in provincia Aragoniae Collegium a Rmo. Illerdensi episcopo erigendum in conventu Oriolae, et donationem ejux juxta decretum Rdi. Provincialis cui in his*

nostram committimus facultatem". The papal bull of 26 September 1562 of Pope Julius III approves the foundation, endowment, and erection of the College of Our Lady of Succour and Patriarch Saint Joseph of Orihuela, with the privilege of a University that grants the academic validity of bachelor, licentiate, and doctorate degrees. The College and the Pontifical University coexisted until the Royal General and Public University was declared in 1655. The State declared it an Artistic Monument in 1864. In 1872, the Society of Jesus (Jesuits) was established and founded a High School which taught until 1956, and from then on the Bishopric of Orihuela took over and it became a Diocesan School and shares a University Seat with the University of Alicante from 1998 to the present day. It was declared a National Historic Monument in 1931 and later declared an Asset of Cultural Interest in the category of Monument according to the Valencian Heritage Law 4/1998.

The Santo Domingo School in Orihuela is one of the most important 16th century architectural complexes in the Valencian Community, both for its layout and for the quality of its execution. Located between Adolfo Clavarana street and the city's Sierra, it has a built surface area of 21,000 m². The building was designed by the architect Jerónimo Quijano in 1552 and 3 of the 4 parts of the original plans and "traces" have been preserved, with the area where the Refectory is located today being precisely missing. The architect Juan Inglés directed the works at Santo Domingo from 1566, after Quijano's death, designing and building the famous staircase that forms part of the complex (Figure 1).

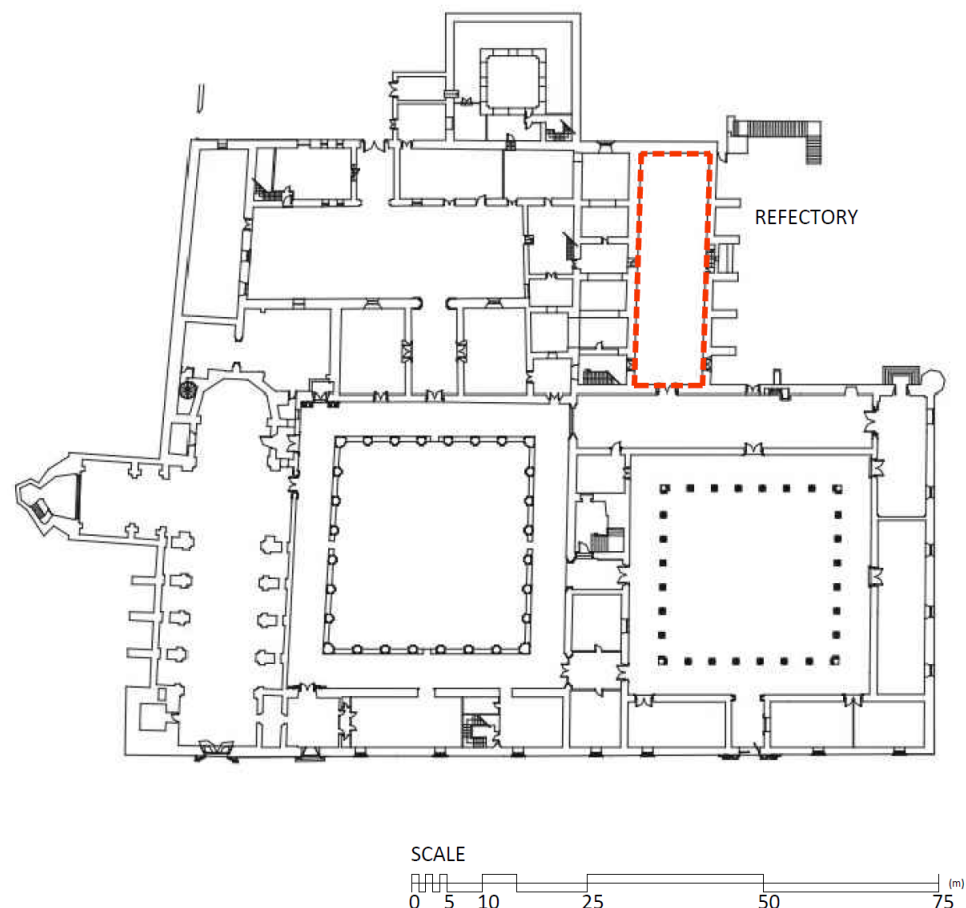


Figure 1. Floor plan of Santo Domingo de Orihuela.

We can highlight some of its architectural elements that define it spatially and formally as characteristic and singular of the complex: Main façade with a marked horizontality interrupted by the three access portals, Church façade (16th century) by Joan Inglés, Convent façade with the three classical orders, Baroque style University façade (early 18th century) by Pedro Juan Codoñer, Church of the Virgin (16th century), Bell Tower (18th

century) which replaces a Renaissance bell tower, Convent Cloister (early 17th century) by Agustín Bernardino, Sacristy façade (late 16th century) by Joan Inglés, University Cloister of Renaissance composition (1727–1737) by Francisco Raimundo and refectory.

The refectory of the college has changed over time, as the building grew and the number of friars and students increased. The needs increased and so the surface area destined for this use underwent successive changes. According to the historian Javier Sánchez Portas, in 1591, payments are documented for the carving of stone for a new refectory that seems to coincide with the current one of one hundred and forty-two palmos (the unit of measurement used in the 16th century) in length and forty-four in width (320 square metres).

The refectory is covered by a ribbed vault with semicircular arches that span the width of the nave and former arches on both longitudinal walls. The north side is finished off with a flared semicircular arch, with geometrical coffers in deviation. The refectory contains a plinth of 18th century Valencian tiles (Manises) that must be protected as an element of great value that forms part of this architectural space.

Work on the refectory may have been completed in 1595. However, the date of 1794 inscribed on the walls of the refectory casts doubt on the real date of execution of this part of the college. This fact further justifies the need to document the restoration work, and to learn about the different construction systems, rooms, and connections that have materialised in the current state of the building.

In 2006, a conservation master plan was drawn up in which several phases of intervention were established, giving priority to the parts of the complex with structural damage. Among these urgent phases of action was the refectory, as it had structural problems with cracks in the vaults and walls. The gabled roof over the upper rooms, built on a wooden structure of par-hilera wood, was also very deteriorated, implying risks of stability on the refectory space, as it resolves its covering, and, therefore, reinforces the need for conservation.

The assessment of intervention needs in historical and heritage buildings requires information and knowledge offered by the application of precise techniques for their registration, which is why it is common practice in the preliminary phase of data collection in architectural restoration projects. Terrestrial laser scanner (TLS) [1,2] and photogrammetry [3–7] are often used as they are techniques that allow the necessary graphic documentation to be obtained with great precision if used appropriately [8–10]. Each building requires individualised treatment, so that, although the methodology is general, its specific application in each case requires adaptation to the particular conditions of the architectural element. In spaces covered with vaults, it is not possible to access the back of the vaults, so the initial record is partially incomplete. However, metric and visual information is necessary to determine the definition of the existing constructive elements: orthogonal graphic views (plans, elevations, and sections), as well as volumetric perspectives are essential for the initial constructive analyses, and for future intervention and maintenance projects. For this reason, and in order to complete the graphic information, it is necessary to complete the data collection during the restoration work in order to document the geometry and construction systems of the building with reliable and quality results [11–15] (Figure 2).

1.1. State of the Art LIDAR and Photogrammetry

LIDAR surveying uses a laser beam to collect information. The technology works by emitting lasers and measuring the time it takes for the light to return to the source. This technique came into use in the 1990s and makes it possible to date the coordinates of the analysed points with respect to the emitter. Photogrammetry collects data by analysing and comparing multiple two-dimensional images (photographs) to create a three-dimensional model. It is considered a passive sensor because it does not produce its own energy source to collect information. Both LIDAR surveying and photogrammetry can be used to take measurements and discern data. LIDAR creates a three-dimensional model through a laser target. The scanning frequency and repetition rate will determine a point cloud.

Photogrammetry produces a fully coloured 3D image by “stitching together” multiple 2D photographs, although it may take thousands of photographs to obtain an accurate model. In this work, data acquisition has been done by combining both techniques: laser scanning and photogrammetry.

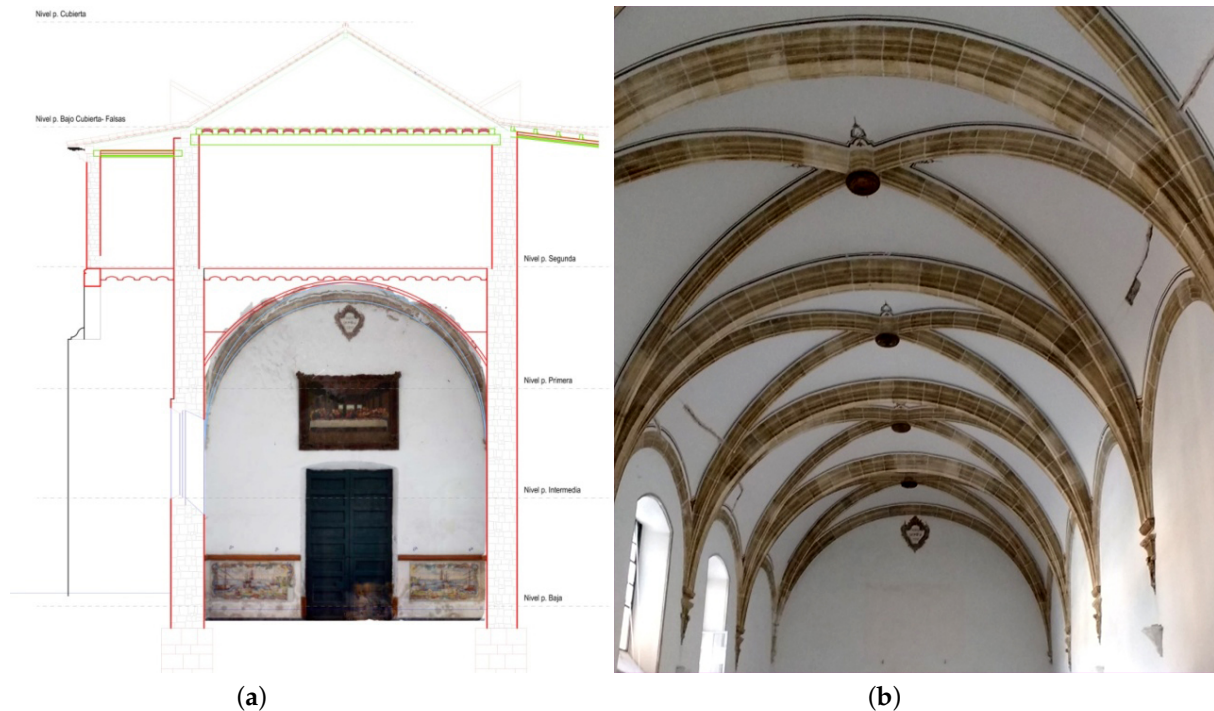


Figure 2. The spatial distribution of arches and vaults in the refectory area. (a) the sketch of vertical cross-section (b) vaults directional arrangement.

2. Methodology

All the data collected with the techniques described (LIDAR using TLS (terrestrial laser scanner), and photogrammetry using SfM (structure from motion)) have been analysed and processed with the Cyclone - Leica (Heerbrugg, Switzerland), 3DReshaper (Neyron, France), and Cloudcompare (Paris, France) software and the plans obtained with CAD programmes (Generic and free programmes), following the following methodology:

2.1. Analysis of Available Documentation

The analysis of the plans is carried out through the Basic and Execution Project of the refectory and classrooms of the Diocesan College of Santo Domingo in Orihuela, as well as the Master Plan of the Santo Domingo College, both documents drawn up by the architect José Antonio Maciá Ruiz.

We encountered some difficulties in the process of reading the information because the different plans have the limitations of data collection from ocular inspections in situ and graphic representations in the views and plans made with CAD programmes [16,17].

The most conflictive situations arise in the definition of those construction elements that are hidden in the walls, vaults, and floors, with evident doubts about the dimensions and location of some systems and their possible injuries.

Historical analysis and knowledge of the different stages of construction that the evolution of the building has undergone is important. For this reason, other sources of information have also been analysed, such as the photographs of the historical school, which are included in some publications, such as “The history of a dream, 50th Anniversary of the Diocesan Management of Santo Domingo School (1956/57-2006/07)” or “Inmaculada-Santo Domingo 20th Century” published by the Jesuit Alumni Association of Alicante, which managed the school from 1867 to 1956.

The maintenance and protection of built heritage implies a record of the known data and its constant updating, recording all the modifications it has undergone throughout its history. The purpose of this article is to contribute to the availability of adequate information on the architectural construction and its chronological evolution, as well as the actions carried out on a heritage asset with the aim of preserving it for the enjoyment of future generations [18,19].

2.2. Description of the Works Defined in the Restoration Project

The main objective of the restoration work is to achieve structural stability and restore both the refectory area on the ground floor and the upper space on the first floor to be used as teaching workshops. The work is being carried out with the supervision and support of a team of archaeologists whose mission is to record and date all the work, and to warn of the importance and constructive decisions that could lead to possible discoveries in the development of the different items to be carried out.

The following is a brief chronological description of the works as defined in the Project and their implementation, reflecting the existing construction systems and the proposals for other alternatives in the restoration process.

1. Prior to the start of the restoration work, unique elements, such as the 18th century tile plinth, which is located around the perimeter of the base of the Refectory, and the mural paintings found both at the head and foot of this single rectangular nave, were protected;
2. Prior to the demolition work on the floor slabs resting on semicircular arches, false-work has been installed to ensure the safety and stability of the vaults and arches;
3. The exterior wall of the refectory is stabilised and consolidated by injecting fluid lime mortar. The existing cracks in the vaults and arches are sealed with special lime mortar and some stitching is carried out with vitrosin rods. The CINTEC ST system was used to tie the walls enclosing the refectory in order to ensure that the separated parts were sewn together. The back of the vaults is reinforced by plastering with PLANITOP HDM Restauro fibre-reinforced bicomponent mortar reinforced with Mapei fibreglass mesh, guaranteeing their uniformity [20–24];
4. Subsequently, the new horizontal frameworks of the second floor (floor slab over the refectory) with one-way floor slabs using laminated wood beams with a double waterproof board beam and a compression layer of 8 cm thick lightened concrete, reinforced with electro-welded mesh, were installed;
5. In the exterior lateral area, adjacent to the refectory, on the buttresses, there are reinforced concrete joist-beam slabs built in situ. All of them are tied perimetrically by means of reinforced concrete strapping and metal profiles, with the aim of organising a perimeter framework tying all the floor slabs both on the arches and on the walls that delimit it (Figures 3 and 4).

2.3. Use of Terrestrial Laser Scanner (TLS) and Structure from Motion (SfM) in the Monitoring of Cultural Heritage Restoration Works

These techniques make it possible to take data on the geometric position of the surfaces of all the elements that form part of architectural construction systems (cladding, masonry, structures...) and of any of their materials (mortars, plaster, stone, ceramics...), knowing their coordinates and offering the possibility of comparing them in the study processes.

In order to obtain a reliable action model, it has been necessary to collect new data in the progress of the works and to compare the information available in the archives with other more current information that served as the basis for the project. This information makes it possible to document the process of the material execution of the construction elements, and to evaluate their behaviour in the face of the different stresses to which they are exposed.



Figure 3. Construction process in the restoration. (a) Original slab floor with horizontal wood joists (b) Falsework for stability guarantee in the works (c) the active vertical fracture along wall and vaults disturb stability of the study complex that must be consolidated.



Figure 4. (a): Slabs using laminated wood beams. (b): Joists-beam concrete slab built in situ.

With the idea of preserving the history of the building, a real geometry of the archaeological and architectural elements must be available, and, therefore, traditional measuring tools, such as the flexometer, levels, and new techniques that provide us with a 3D point cloud acquired from laser and photogrammetry, and that specify the shape and dimensions of the existing materials and construction systems, have been used.

For the recording, study and monitoring of the vaults and arches of the refectory, in the different stages analysed, and given their sometimes difficult accessibility, we have opted for the use of digital tools. On the one hand, through the use of terrestrial light detection and ranging technology [24] (LIDAR) using a high-precision laser scanner [25] for data collection, its subsequent graphic survey and virtualisation in three dimensions using the Cyclone, 3DReshaper, and Cloudcompare software [26], and the capture of high-resolution images.

The laser scanner used is a pulsed time-of-flight laser scanner, Leica ScanStation C10 model, which measures a laser beam generating a point cloud of the scanned element with a maximum density of one point every 2 mm of distance, a complete field of vision of 360° horizontally and 270° vertically, with a long range (up to 300 m).

On the other hand, SfM photogrammetry [27,28] is employed, with digital photography by taking photographs using a Canon EOS 600D SLR camera with a Canon EF-S 18–55mm standard lens. The photographs were processed using Photoscan software and metashape [29–34] (Figure 5).

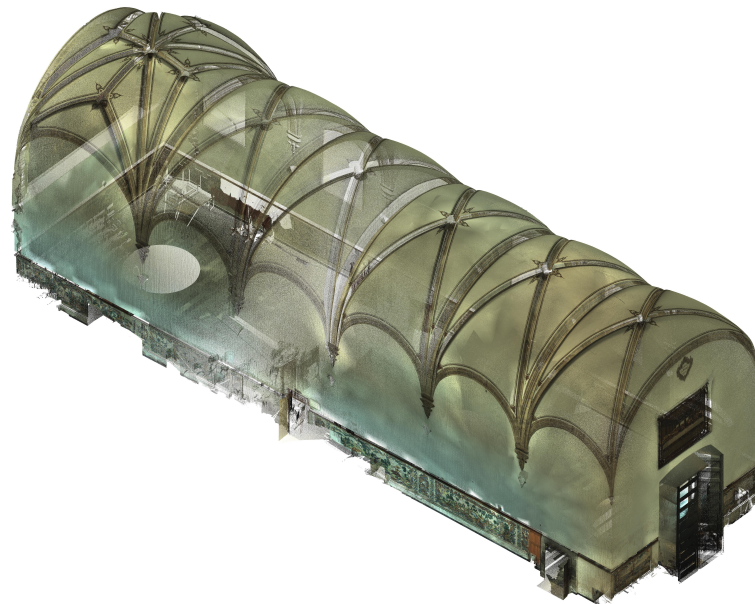


Figure 5. Top axonometric view of the geometrical vaults arrangement.

Data collection with the Laica Scan Station C10 Laser Scanner was carried out at different times, before the start of the works (2015) and after completion of the works (2019), choosing a position centred in the Refectory on a tripod, so that the scanning distances were, at most, of the order of 15 m. The intermediate state of the works was recorded with six locations on different dates (2018 and 2019) given that the demolition and reconstruction process took place in different phases, each one corresponding to each span (five arches and six vaults). Similarly, and coinciding with the days on which it was scanned, the state of the work was also recorded with the Canon 600D SLR digital camera. Using the Cyclone Leica software for cloud recording and 3DReshaper for cloud analysis and deformation control, the point cloud obtained from the different scans was processed, and above all, the “Cloudcompare” software was used to analyse the data from the different states of the work, taking certain characteristic points as a reference, and carrying out verification tests so that the distances between them were constant in the stages compared. After taking the data by means of on-site scanning, the point clouds and the images were made compatible using Photoscan and Metashape software, in order to visualise them using orthophotos, which can be scaled based on the measurements obtained from the point cloud; in all cases, photogrammetric work was carried out in which each image coincided at least 50% with the previous one, defining characteristic points (which remain invariable throughout the construction process) in such a way that the key points can be recognised from the image to the point cloud, obtaining all the graphic data that record the process. Once the definitive positions of the compared point clouds had been defined, and with the same reference coordinate system, the data were exported to AutoCAD files. Finally, the data of the analysed points are transferred from Cloudcompare to AutoCAD, showing the x , y coordinates of each of the compared points. The point cloud was divided by means of strips parallel to the segmental arches to make a section on the axis of each of

them (Figure 6). The arches are made of limestone voussoirs whose surface is the result of the original tiling work (without facing), so that the data obtained in the scan reflects small irregularities resulting from the stone micro-grains that generate an envelope with small jumps between the points (Figure 7). The process implies an error in the measurements that can be estimated to be in the order of 2 mm (distance between the scanning points and irregularities of the sectioned surface), so it can be considered acceptable as we are in a range of measurements of less than 1/1000 of the span of the arc.

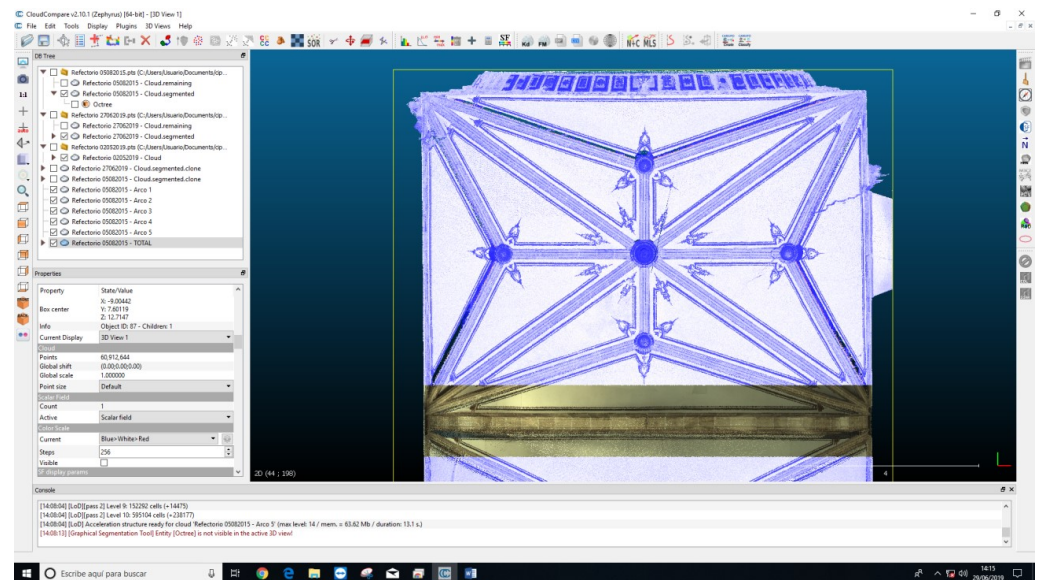


Figure 6. Strip corresponding to one arches studied with CloudCompare V2.10.1 software.

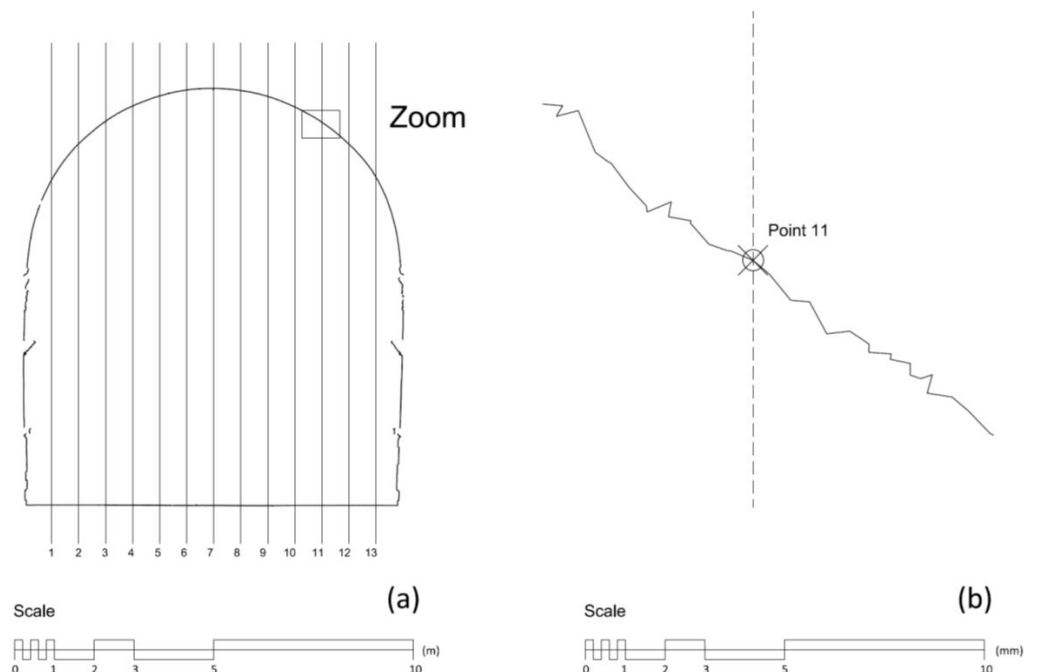


Figure 7. Graphic representation of standard arch coordinates points offered in Table 4 (a) the arch is divided in 14 equidistant sections including the key (b) a point zoom of the lower arch path to obtain the coordinates (x,y) with the AutoCad program.

2.4. Description of the Different Stages Considered in the Benchmarking Study

The use of these digital tools has been proposed for the documentation and monitoring of the restoration process of the refectory [30] in 3 stages, analysing various points of

the cross-section of the transverse arches, and at the same time comparing the results between the different spans analysed, so that the different points observed and the three stages considered are different and comparable, from the initial state of the works to their completion. To complete the study, an estimate is made of the state of loading of the structure in each of the phases analysed [35].

Data were taken prior to the intervention using the point cloud provided by the technique used, and the data are reflected in a graphic representation of different sections that allow us to analyse both the dimensions of the different construction systems and the deformations and displacements produced [14,36], in the arches-nerves as well as in the vaulting-plementeries.

The information is completed with the load states in each of the stages, which give us an idea of the stresses to which they are exposed and the response of the construction solutions before, during and after the intervention.

- Stage 1 (2015): This is the phase of the studies prior to the restoration project with the aim of preparing a diagnostic study; the building is scanned with a laser scanner in order to graphically record the initial state of the construction elements prior to the drafting of the project, prepare exact planimetries and, from the cloud of points generated, study deformations, detect pathologies, and analyse the structural behaviour that will allow us to hypothesise the situation of the building and the origin of the damage observed.

In this pre-existing situation, the segmental arches have been subjected to the same loads for more than 400 years, typical of the traditional construction system: the weight of the arch itself, solid brick masonry, one-way wooden joist floor slabs with brick revolts and floors laid with hydraulic mortar.

- Stage 2 (year 2018): During the restoration works, the different phases of the execution of the project are scanned with a laser scanner, demolition of partitions and floors, unloading of vaults... Any change or constructive and structural modification to observe by comparison with the point cloud of phase 1, the changes that the vaults may be suffering. In this phase, we obtain the record of the vaults' backsides, allowing us to obtain their thickness and study their construction system and structural behaviour. It is not possible to scan the soffit as it is propped up.

In this phase, SfM photogrammetry is used to document and record the different constructive actions, surfaces brought to light, as well as the structural reinforcements made to the vaults that are hidden at the end of the restoration [37].

The data are transferred, which in this case corresponds to the unloaded arches and vaults, as the floors and their corresponding pavements have been demolished.

At this stage, the moment analysed collects the information at the moment when the partition walls, floors, and ceramic revolts have been demolished and the wooden joists have been removed, so that the floor slab has disappeared. We can consider that this is the moment when the structure formed by arches and vaults is unloaded and only subjected to its own weight (Figure 8).

- Stage 3: A terrestrial laser scan of the final state of the work after its restoration is carried out. This scan allows us to compare the point clouds of the initial state in Phase 1 and the final state in Phase 3, as well as to have the final geometry of the building. The scan provides information on the soffit of the arches and vaults, and the initial and final state of the arch guidelines can be compared.

In this phase, the forging is executed again, but in this case with a different system, based on a unidirectional framework of wooden joists with a double board supporting a compression layer of lightened reinforced concrete and finished with wooden flooring, having reinforced the vaults and the upper wall of the arches with mortar and metal profiles; and all of this results in a state of loads very similar to the initial state.

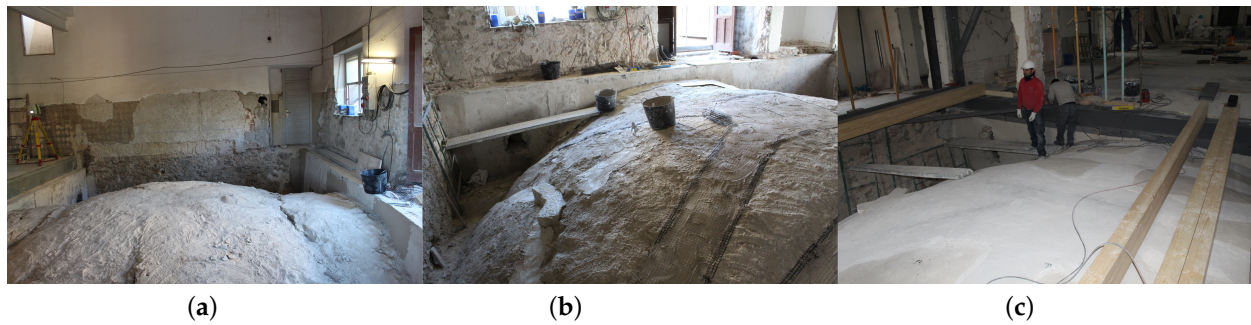


Figure 8. Principal vault extrados on its different restoration states: (a) Original (b) Reinforcement application on nerves (c) Finished.

2.5. State of Loads in the Different Stages of the Process

The criterion used to analyse the behaviour of the vaulted structure of the Refectory is the comparison of the state of loads and deformations in each of the defined stages [3,35] and in two different situations: on the one hand, we have considered the segmental arches (arches 1, 2, 3, and 4), which are stressed by vaults, walls, and floors of similar dimensions and construction solutions, and on the other hand, arch number 5, which receives the loads from a different floor and vault surface, since the span of the last span is greater.

In the transverse arches, two different points have been considered: the keystone (K) in the centre of the arch and the salmeres (S) at the extreme supports.

For this purpose, the weights of the elements involved in the construction system are taken into account, based on the data provided in the tables of Annex C, Basic Document SE-AE of the CTE [38]:

- **Dead weight of the vault**, built with two threads of solid brick taken with lime mortar and rendered on the top and bottom with the same mortar, with an average thickness of 12 cm, and the consideration that the dead weight of a solid brick masonry with lime mortar is 18 KN/m^3 , which results in: $Q_{\text{vault}} = 0.12 \text{ m} \times 18 \text{ KN/m}^3 = 2.16 \text{ KN/m}^2$. A load band is considered in the keystone (Q_k), of 2 m for the standard arch and 1.5 m for arch 5. In the salmeres (Q_s) is not considered, given that the vault discharges on the former arches and the lateral wall;
- **Dead weight of the unidirectional slab** resting on the brick masonry in segmental arches, made up of timber beams, beamwork based on solid brick revoltón and hydraulic tile paving on fillings and lime mortar. An average thickness of 15 cm and a density of 18 KN/m^3 has been considered, and for the timber an average density of 8 KN/m^3 , so that we can estimate an initial slab weight of 3.30 KN/m^2 for the initial slab. A constant load band of 5 m is considered for the standard arch and 6 m for arch number 5;
- **The dead weight of the 1 foot brickwork** (Catalan format with approximately 30 cm of rope) on the segmental arches is $Q_{\text{brickwork } 1 \text{ foot}} = 5.4 \text{ KN/m}^2 \times h$. This load is variable, being minimum on the keystone $Q_{\text{keystone}} = 5.4 \text{ KN/m}^2 \times 0.25 \text{ m} = 1.35 \text{ KN/m}$ and maximum on the starts $Q_{\text{factory start}} = 5.4 \text{ KN/m}^2 \times 2 \text{ m} = 10.8 \text{ KN/m}$, considering the studied points C and S, respectively;
- **Self-weight of the rib-arches** made of limestone with a cross-section of approximately $0.20 \text{ m} \times 0.40 \text{ m}$ would have a uniformly distributed linear load of $Q_{\text{rib-arches}} = 0.20 \text{ m} \times 0.40 \text{ m} \times 28 \text{ KN/m}^3 = 2.24 \text{ KN/m}$, considered constant over the entire arch (Figure 9);
- **Overloading of partition walls.** The floor above the refectory is very diaphanous, with a partition wall of hollow brick with a thickness of 10 cm, and for this purpose a uniformly distributed linear load of 5 KN/m is considered. This is why this situation is considered to be the standard arch. In arch 5, given its initial situation with less partition walls, a load of 2 KN/m is considered.

In the first phase, the state of charge results about original materials and elements (Table 1, Figure 10):



Figure 9. (a): Typical cross-section of the transverse arches. (b): transverse and diagonal arches (in addition to the former arches).

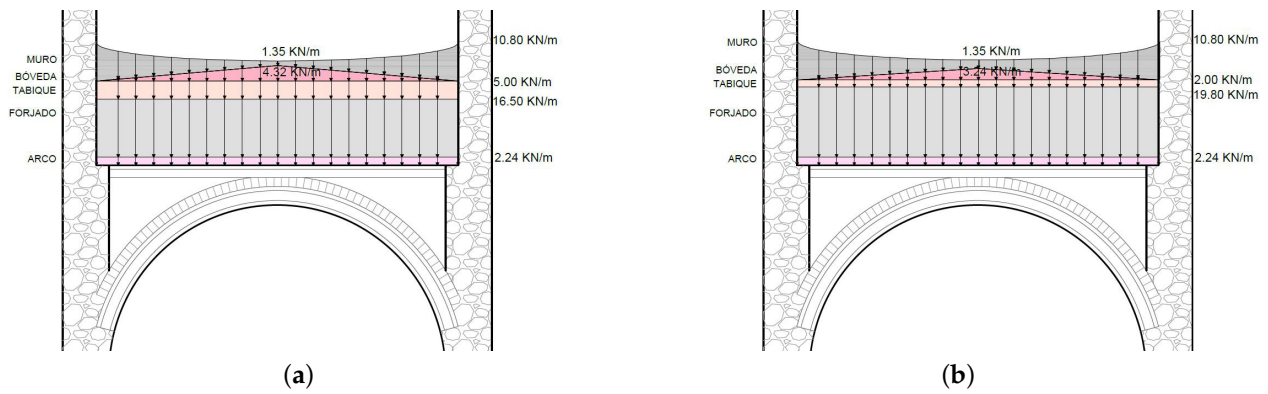


Figure 10. Initial state force diagram (a): arcs 1, 2, 3, and 4; (b) arc 5.

Table 1. State of loads in the initial stage.

Arches Initial State (STAGE 1)	Loads KN/m	Arc KN/m	Floor slab KN/m	Partition KN/m	Vault KN/m	Wall KN/m	Total Load KN/m
Arches 1-2-3-4	Q_k	2.24	16.5	5.00	4.32	1.35	29.41
	Q_s	2.24	16.5	5.00	-	10.8	34.54
Arc 5	Q_k	2.24	19.8	2.00	3.24	1.35	28.63
	Q_s	2.24	19.8	2.00	-	10.8	34.84

In the second phase considered, the initial slab and the partition walls have been demolished, and, therefore, the load state will correspond to the sum of the own weights of arches, walls over arches, and vaults (Table 2, Figure 11).

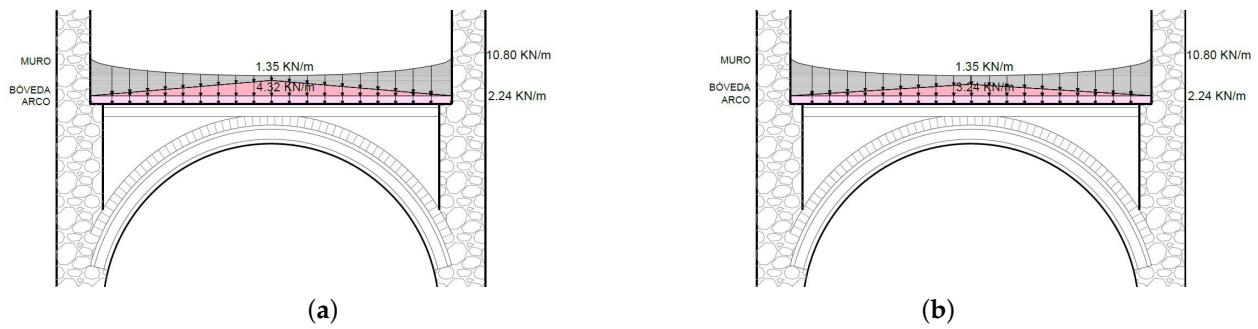


Figure 11. Force diagram of the intermediate state (a): arcs 1, 2, 3, and 4; (b): arc 5.

Table 2. State of loads in the intermediate stage.

Arches Initial State (STAGE 2)	Loads KN/m	Arc KN/m	Floor slab KN/m	Partition KN/m	Vault KN/m	Wall KN/m	Total Load KN/m
Arches 1-2-3-4	Q_k	2.24	-	-	4.32	1.35	7.91
	Q_s	2.24	-	-	-	10.8	13.04
Arc 5	Q_k	2.24	-	-	3.24	1.35	6.83
	Q_s	2.24	-	-	-	10.8	13.04

In the third phase, the definitive state of the loads will be the weight of the new slab and its paving and the reinforcement based on a 2 L 140 metal section as the top of the one-foot wall above the transverse arches. In addition, the reinforcements on vaults and walls are considered (Table 3, Figure 12).

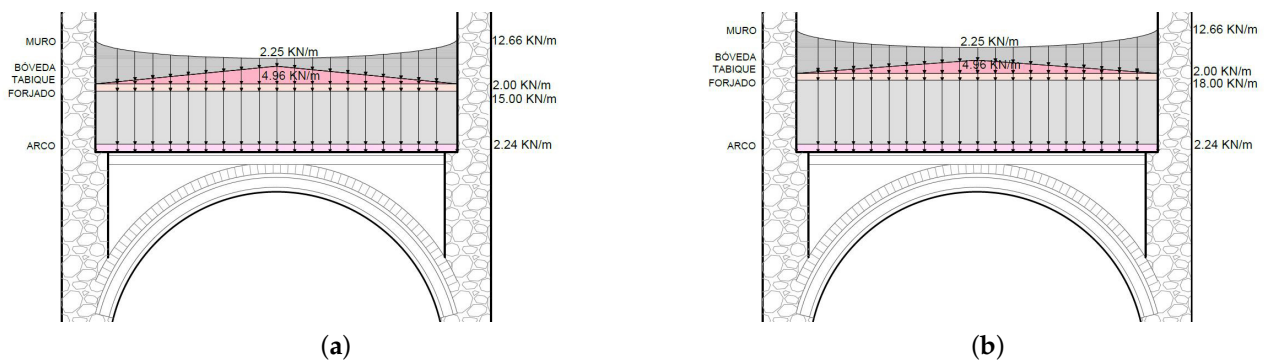


Figure 12. Final state force diagram (a): arcs 1, 2, 3, and 4; (b): arc 5.

Table 3. State of loads in the final stage.

Arches Initial State (STAGE 3)	Loads KN/m	Arc KN/m	Floor slab KN/m	Partition KN/m	Vault KN/m	Wall KN/m	Total Load KN/m
Arches 1-2-3-4	Q_k	2.24	15.00	2.00	4.96	2.25	26.45
	Q_s	2.24	15.00	2.00	-	12.66	31.90
Arc 5	Q_k	2.24	18.00	2.00	3.72	2.25	28.21
	Q_s	2.24	18.00	2.00	-	12.66	34.90

This results in a uniformly distributed excess linear load of $2 \times 0.29 \text{ KN/m} = 0.58 \text{ KN/m}$ due to the load of the metal reinforcement. We also have to take into account an average load of 2 cm thick reinforcement mortar with carbon fibre, assuming a density of 16 KN/m^3 , resulting in a linear load at the keystone of $16 \text{ KN/m}^3 \times 0.02 \text{ m} \times 1 = 0.32 \text{ KN/m}$, and at the starts $16 \text{ KN/m}^3 \times 0.02 \text{ m} \times 2 \times 2 = 1.28 \text{ KN/m}$, which added to the steel structure results in a linear load of the reinforcement elements on

the wall of the arches of $Q_{\text{keystone reinforcement}} = 0.58 \text{ KN/m} + 0.32 \text{ KN/m} = 0.9 \text{ KN/m}$, and $Q_{\text{salmer reinforcement}} = 0.58 \text{ KN/m} + 1.28 \text{ KN/m} = 1.86 \text{ KN/m}$.

As for the new load of the slab, it is made up of new laminated wood beams, a double waterproof plywood board, an 8 cm thick compression layer of concrete lightened with arlite and reinforced with mesh, on which a 5 cm thick self-levelling mortar is placed, and a wooden floor. All this means that the final slab has a surface load of $Q_{\text{final slab}} = 3.00 \text{ KN/m}^2$. The load bands are identical to the previous ones.

In addition, the top surface of the vault has been reinforced with the same mortar and carbon fibre, and an average thickness of 2 cm, which increases the surface load of the vault by $Q_{\text{vault reinforcement}} = 16 \text{ KN/m}^3 \times 0.02 \text{ m} = 0.32 \text{ KN/m}^2$. The load bands considered are the same as above.

In the project, mobile partitions are proposed that will hang from the existing roof support structure, but in some cases (arches 1 and 5) a new division is made based on self-supporting lattice panels, which means a linear load of 2.00 KN/m .

Therefore, the initial and final load states are similar.

2.6. The Stress Response of the Structure by a Simplified Model

In order to understand the structural behaviour of the system, based on the loads considered, a simplified modelling is proposed based on the study of the mechanical behaviour of the splay arches, which are the final receivers of the load system.

Considering the arch as a tri-articulated isostatic structure (Figure 13), we can calculate the support reactions from the three equations of plane statics [39–41].

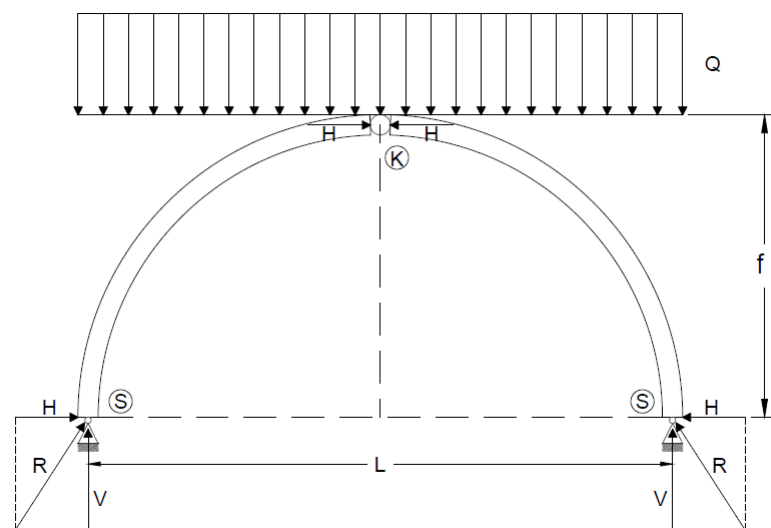


Figure 13. Tri-articulated isostatic arch. Graphical sketch of tri-articulated isostatic arch. (S= salmer, support stone; K= keystone; L= light of the arch; H= horizontal reaction; V=vertical reaction; R= Resultant reaction; Q= linear distributed load; f= deflection of the arch).

For this purpose, we model uniformly distributed loads in each of the three cases studied, choosing the most unfavourable situation. The system will reflect maximum horizontal reactions in the keystone and vertical reactions in the brackets, so that the resultant at the start of the arch originates the stresses that it must absorb [42].

Where Q (KN/m) is the uniformly distributed load considered in each case; L (m) is the span of the arch and f (m) is the deflection or edge of the arch; H (KN) (horizontal reaction at the keystone, which is equal to that of the supports so that the system remains in equilibrium) and V (KN) (equal vertical reaction at the two supports), at the three articulated points of the system (keystone and two supports); R (KN) (resultant of the vertical and horizontal components at the supports); and according to the equations of statics, the horizontal reactions are obtained:

$Q \cdot \frac{L}{2} = H \cdot f$; $H = Q \cdot \frac{L^2}{8 \cdot f}$ and the vertical reactions would be $V = Q \cdot \frac{L}{2}$

We can obtain the Resultant on the supports $R = \sqrt{H^2 + V^2}$

For each of the stages analysed and studying the worst case for each of them,

STAGE 1. The largest uniformly distributed load is $Q_1 = 35$ KN/m, so the following is obtained

$H_1 = Q_1 \cdot \frac{L^2}{8 \cdot f} = 83.12$ KN; and the vertical reactions would be $V_1 = Q_1 \cdot \frac{L}{2} = 166.25$ KN

We can obtain the resultant in the supports $R_1 = \sqrt{H_1^2 + V_1^2} = 185.871$ KN, so that the maximum stress to which the segment is subjected at the support (salmer) during the initial state of the works, that is, in its four hundred years of service life, is $\sigma_1 = \frac{185,871}{400 \times 200} = 2.32$ MPa = 2.32 (N/mm²).

STAGE 2. The largest uniformly distributed load is $Q_2 = 13$ KN/m, so we obtain

$H_2 = Q_2 \cdot \frac{L^2}{8 \cdot f} = 30.87$ KN; and the vertical reactions would be $H_2 = Q_2 \cdot \frac{L}{2} = 61.75$ KN

We can obtain the resultant at the supports $R_1 = 69.036$ KN. $\sqrt{H_1^2 + V_1^2} = 69.036$ KN, so that the maximum stress to which the segment is subjected at the support (salmer) at the moment when the slabs have been demolished is $\sigma_1 = \frac{69,036}{400 \times 200} = 0.86$ MPa = 0.86 (N/mm²).

STAGE 3. The highest uniformly distributed load is $Q_3 = 35$ KN/m, which coincides with one of the most unfavourable states in which the initial state of loading (Stage 1) was found, so the same results are obtained, and, therefore, once the restoration work has been completed, the maximum stress to which the voussoir is subjected at the support (salmer) is $\sigma_3 = \frac{185,871}{400 \times 200} = 2.32$ MPa = 2.32 (N/mm²).

The compressive strength of the limestone used to make the arches has not been tested, but according to the examples consulted [43,44], we can consider a minimum admissible stress of 10 N/mm² (MPa), and for the lime mortar in the joint of the voussoirs of 10 N/mm².

According to Annex C. of the Basic Document SE-F [38], the characteristic compressive strength f_k in N/mm² of the masonry, considering the arch as such, can be calculated with the equation:

$$f_k = K \times f_b^{0.65} \times f_m^{0.25} = 0.6 \times 10^{0.65} \times 10^{0.25} = 4.76 \text{ N/mm}^2 = 4.76 \text{ MPa}$$

Applying the DB-SE-F criteria of the CTE [38], a reduction factor of 0.9 is considered, equivalent to an eccentricity of 5% of the thickness of the arch (20 mm), and, therefore, the geometric section equivalent to the compressed area would be 90% of the real one, so that in the worst case (when the restoration work has been completed), 2.32 MPa / 0.90 = 2.57 MPa < 4.76 MPa. = 4.76 (N/mm²).

2.7. Deformations

Throughout the process described in the three stages considered, the graphic documentation of the arches has been recorded, based on the point clouds obtained at the beginning (Stage 1) and at the end of the works (Stage 3). In the intermediate stage (Stage 2), the soffits of arches and vaults were found with falsework guaranteeing their stability in the demolition phase (only the soffit was scanned), representing the elevations obtained in each of the cases and with the means and techniques already mentioned (Figure 14):

The coordinates (height) of each of the points observed in the comparison of the 5 arches analysed before (2015) and after (2019) the works are shown below (Table 4 and Figure 7). Having established the position of a certain point (always the same) in each of the keys clearly referenced to another point fixed in the space of the refectory and without any possibility of movement, in order to take the measurements that register the possible differential movements in three-dimensional coordinates of one stage with respect to the other.

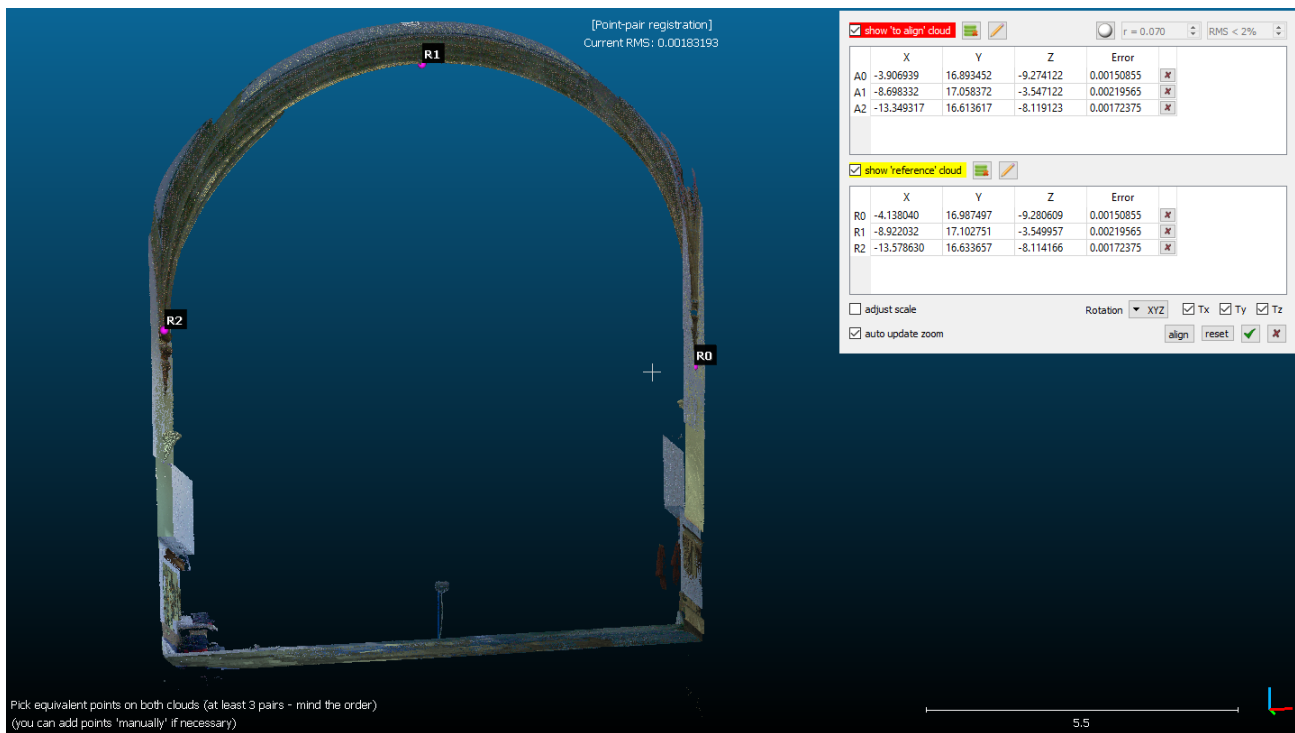


Figure 14. The ordinates are obtained, at least, with 3 fixed reference points (R_0 , R_1 , R_2) in the arches studied with CloudCompare software.

Table 4. Comparison of all arcs.

Arc	1	2	3	4	5	6	7 Key	8	9	10	11	12	13
Arc 1													
Stage 1	8.067	8.966	8.538	9.916	10.162	10.299	10.343	10.301	10.162	9.913	9.523	8.953	8.055
Stage 3	8.066	8.968	8.537	9.917	10.163	10.304	10.344	10.298	10.158	9.909	9.521	8.948	8.032
Descent	0.001	-0.002	0.001	-0.001	-0.001	-0.005	-0.001	0.003	0.004	0.004	0.002	0.005	0.003
Arc 2													
Stage 1	7.893	8.819	9.445	9.848	10.116	10.259	10.312	10.263	10.119	9.873	9.489	8.863	7.902
Stage 3	7.892	8.819	9.445	9.847	10.108	10.252	10.303	10.256	10.113	9.866	9.481	8.856	7.894
Descent	0.001	0.000	0.000	0.001	0.008	0.007	0.009	0.007	0.006	0.007	0.008	0.007	0.008
Arc 3													
Stage 1	7.88	8.865	9.462	9.859	10.113	10.249	10.307	10.263	10.113	9.873	9.503	8.923	7.994
Stage 3	7.882	8.862	9.460	9.855	10.108	10.246	10.302	10.262	10.106	9.866	9.494	8.913	7.989
Descent	-0.002	0.003	0.002	0.004	0.005	0.003	0.005	0.001	0.007	0.007	0.009	0.010	0.005
Arc 4													
Stage 1	7.984	8.95	9.525	9.926	10.204	10.357	10.387	10.340	10.206	9.966	9.586	9.027	8.151
Stage 3	7.992	8.956	9.529	9.927	10.204	10.350	10.387	10.335	10.203	9.966	9.575	9.018	8.144
Descent	-0.002	-0.003	-0.004	-0.001	0.000	0.007	0.006	0.005	0.003	0.000	0.011	0.009	0.007
Arc 5													
Stage 1	8.194	9.101	9.672	9.062	10.322	10.476	10.514	10.462	10.317	10.045	9.658	9.110	8.263
Stage 3	8.190	9.096	9.671	9.064	10.322	10.476	10.511	10.464	10.313	10.045	9.657	9.111	8.265
Descent	0.004	0.005	0.001	-0.002	0.000	0.000	0.003	0.000	0.004	0.000	0.001	-0.001	-0.002

The five arches analysed are divided into 14 equidistant sections and 13 points are studied, including the keystone and excluding the salmeres, which are considered fixed. The coordinates on the X axis are equidistant and the coordinates on the Y axis correspond to the height above the ground line plane (the same in all cases) up to the soffit of the arch axis (described in Section 2.3) which contains irregularities due to the surface of the stone voussoirs and the error inherent to the technique used (point cloud).

The data obtained range from -0.005 m (rise of point 6 of arch 1) to 0.011 m (fall of point 11 of arch 4), reflecting minimum movements of all the arches studied. The deformations produced at point 3 of all the arches (kidneys facing the interior zone of the building) range from -0.004 m in arch 4 to 0.001 m in arches 1 and 5; the deformations at point 11 of the arches (kidneys in the exterior zone of the refectory) vary from 0.001 m in arch 5 to 0.011 m in arch 4; the kidneys of the inner zone, west of the refectory, descend less than the east zone; the movement of the keystones varies from -0.001 m in arch 1 to 0.009 m in arch 2, being in this case also a small descent.

Given the relative error in the data collection, where the sensitivity of the measurements is in the order of 2 mm, we can consider that there has been hardly any movement in the keystones and kidneys of the arches.

Movements have been observed both in the vaults and in the diagonal rib arches, and some cracks and displacements of construction elements have been observed, even some detachments in fragments of vaults; information that was already included in the Master Plan of the Santo Domingo School: "it has been observed that the upper slab is occasionally supported by pilasters on the vault's backside...", but these movements have not affected the transverse arches studied (Figure 15).



Figure 15. (a): Downturned voussoirs of diagonal arches. (b): Deformations and cracks in vaults.

Nor has any differential movement been observed in the arch supports where they meet the perimeter walls.

3. Discussion of Results

The use of TLS and SfM in the monitoring of the restoration works of the Refectory of the Santo Domingo College has made it possible to record its geometry accurately, as well as to document graphically all the walls and construction elements that have been intervened during the works.

The point cloud obtained in the intermediate stage, once the pre-existing floors have been demolished, provides data on hidden construction elements: the vault is 11 and 12 cm thick (Figure 16). In the same sense, the recording of all the data collected in the intervention process makes possible the archaeological analysis and the study of possible findings. An important debate is opening up that relates the compatibility of traditional construction models and construction systems used in retrofitting that respect the heritage received [45,46] and the standards of quality and structural safety [47]. Comparison of the initial loads (34.54 KN/m in the starts of arches 1, 2, 3, and 4; and 34.84 KN/m in the start of arch 5) with the final loads (31.90 KN/m at the start of arches 1, 2, 3, and 4; and 34.90 KN/m at the start of the arch 5) confirm a final load state that is more favourable or equal to the initial one. The loads on the keys offer a similar conclusion (initial loads of 26.45 KN/m in arches 1, 2, 3, and 4; and 28.63 KN/m in arch 5) and (final loads of 26.45 KN/m in arches 1, 2, 3, and 4; and 28.21 KN/m in arch 5). The data obtained in (Table 4) show a maximum deflection of 11 mm, so that the deflections are negligible and less than the deflections allowed in conventional slabs. The deflections in the arch kidneys

in the West zone of the Refectory (approximate point 3 of the arch), with a maximum of 2 mm, are smaller than in the East zone (approximate point 11) with a maximum of 11 mm, which indicates a tendency to greater movements in the parts of the arches closest to the façade (exterior).

As a working methodology to be followed in restorations similar to the one shown in this work, the use of digital tools is proposed for the documentation and monitoring of the restoration process in the 3 phases of work: in the preliminary studies, in the execution of the works and in the final state of the restoration.

The point cloud obtained at the end of the works is checked against the initial one to study possible differential movements [3].

The decreases recorded are negligible, so that we are in the order of $f < 1/1000$ of light, less than the deflections required for slabs in buildings, and probably due to the commissioning of the new state of loads on the previously dismantled structure.

The recoveries in the deformations of the vaults not addressed in the present investigation may be the subject of future studies. In some cases they may be the result of cleaning and adjustment of some of the voussoirs.

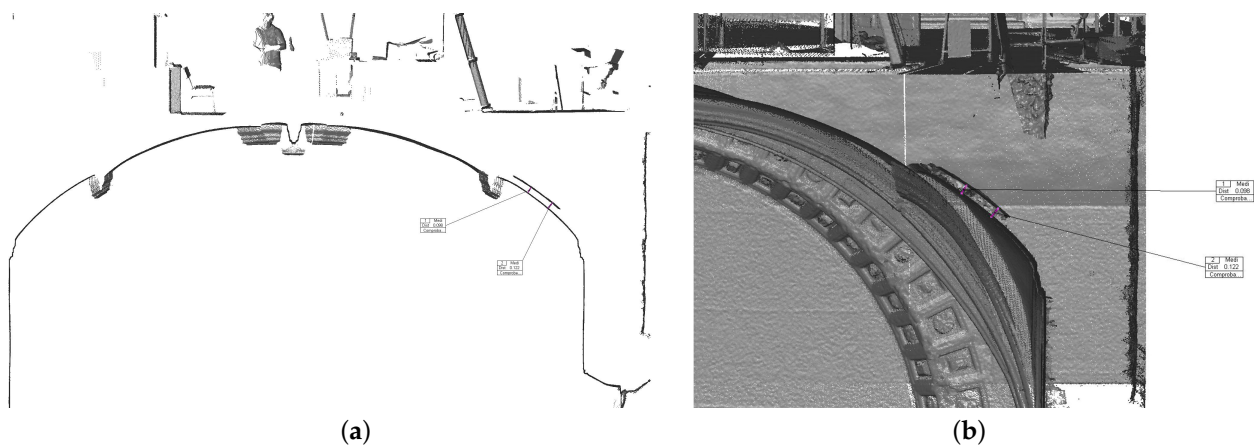


Figure 16. Point cloud section during the restoration works. (a) The measure of the vault section can be obtained. (b) In detail.

4. Conclusions

The laser scanner and photogrammetry techniques used are fundamental for the processes of data collection prior to the project, monitoring the works and the final result with the aim of recording the architectural and heritage object, preserving its condition, and guaranteeing its maintenance. The analysis of the graphic information obtained has generated and historical and documentary research is necessary for the knowledge of the building and the construction procedures that led to its execution. The relevant role of the structural behaviour of the construction solutions incorporated in the project and their behaviour in the chronology of the work, as well as the comparison between the initial and final service states.

The work on the Refectory reinforces the structure of the building on the one hand and simultaneously reduces or equalises the permanent loads by replacing the old heavy slabs with lighter ones. These modifications in the state of the loads produce less or equal stresses in the masonry and vaults of the building, which have a negligible influence on their deformations. The aim of this restoration is to obtain a more stable structural ensemble and better conditions for the maintenance and durability of the construction systems. The analysis of the process in the execution of the works has considered a detailed study of the gravity loads of the different construction systems and their influence on the structural behaviour of the whole.

The techniques for reinforcing vaults, arches and walls at the back improve their stability, and the upper strapping elements improve the load distribution conditions that guarantee greater safety for the structural models proposed.

The techniques and methods used have been able to identify the elements, layers, dimensions, and composition of the materials, as well as the definition of the systems and technology in the construction of the building, to preserve the historical and architectural knowledge of the heritage. The data collected and the reference point clouds for this work generate reliable recorded information to compare and analyse possible future movements of the building.

Author Contributions: Conceptualization, P.S.-G.; Data curation, S.S.-B.; Formal analysis, P.S.-G. and Y.S.-B.; Investigation, P.S.-G.; Methodology, P.S.-G.; Project administration, Y.S.-B.; Resources, J.A.H.-T. and S.S.-B.; Software, J.A.H.-T. and C.R.-M.; Validation, Y.S.-B. and C.R.-M.; Visualization, J.A.H.-T. and C.R.-M.; Writing—review editing, C.R.-M. All authors have read and agreed to the published version of the manuscript.

Funding: This research received no external funding.

Institutional Review Board Statement: Not applicable.

Informed Consent Statement: Not applicable.

Data Availability Statement: Not applicable.

Acknowledgments: Our thanks to the Director of the Diocesan School of Santo Domingo de Orihuela, José María Fernández-Corredor Soriano, and the Administrator Tomás Angel Carrillo; to the Diocese of Orihuela Alicante, promoter of the works that has made possible the development of this research; to the University of Alicante that has provided the technical means for the monitoring and recording of the data obtained by the Scanner; and to the construction company Lorquimur for facilitating the studies carried out during the material execution of the works.

Conflicts of Interest: The authors declare no conflict of interest.

References

1. Pérez-Álvarez, R.; de Luis-Ruiz, J.M.; Pereda-García, R.; Fernández-Marotoand, G.; Malagón-Picxoan, B. 3D Documentation with TLS of Caliphal Gate (Ceuta, Spain). *Appl. Sci.* **2020**, *10*, 5377. [[CrossRef](#)]
2. Suchocki, S. Comparison of Time-of-Flight and Phase-Shift TLS Intensity Data for the Diagnostics Measurements of Buildings. *Materials* **2020**, *13*, 353. [[CrossRef](#)]
3. Dlesk, A.; Uueni, A.; Vach, K. From Analogue to Digital Photogrammetry: Documentation of Padise Abbey in Two Different Time Stages. *Appl. Sci.* **2020**, *10*, 8330. [[CrossRef](#)]
4. Barrile, V.; Bilotta, G.; Lamari, D.; Meduri, G.M. Comparison between techniques for generating 3D models of cultural heritage. *Recent Adv. Mech. Mechatron. Civ. Chem. Ind. Eng. Math. Comput. Sci. Eng. Ser.* **2015**, *49*, 140–145.
5. Giuliano, M.G. Cultural Heritage: An example of graphical documentation with automated photogrammetric systems. *Int. Arch. Photogramm. Remote Sens. Spatial Inf. Sci.* **2014**, *XL-5*, 251–255. [[CrossRef](#)]
6. Kraus, K. *Photogrammetry*; Dümmler: Bonn, Germany, 1993; Volume 2.
7. Luhmann, T.; Robson, S.; Kyle, S.; Harley, I. *Close Range Photogrammetry; Principles, Techniques and Applications*; Chapter 3.3.1.3; Whittles Publishing: Scotland, UK, 2006; pp. 140–141.
8. Mañana-Borrazás, P.; Rodríguez Paz, A.; Blanco-Rotea, R. Una experiencia en la aplicación del Láser Escáner 3D a los procesos de documentación y análisis del Patrimonio Construido: su aplicación a Santa Eulalia de Bóveda (Lugo) y San Fiz de Solovio (Santiago de Compostela). *Archaeol. Archit.* **2008**, *5*, 15–32. <http://dx.doi.org/10.3989/arq.arqt.2008.87>.
9. Vacca, G.; Deidda, M.; Dessi, A.; Marras, M. Laser scanner survey to cultural heritage conservation and restoration. In Proceedings of the International Archives of the Photogrammetry, Remote Sensing and Spatial Information Sciences, XXII ISPRS Congress, Melbourne, Australia, 25 August–1 September 2012; Volume XXXIX-B5.
10. Yastikli, N. Documentation of cultural heritage using digital photogrammetry and laser scanning. *J. Cult. Herit.* **2007**, *8*, 423–427. [[CrossRef](#)]
11. Nieto, E.; Moyano, J.J.; García, A. A. Construction study of the palace of children of don Gome (Andújar, Jaen), managed through the HBIM project. *Virtual Archeol. Rev.* **2019**, *10*, 84–97. [[CrossRef](#)]
12. Massafra, A.; Prati, D.; Predari, G.; Gulli, R. Wooden truss Analysis, Preservation Strategies, and Digital Documentation through Parametric 3D Modeling and HBIM Workflow. *Sustainability* **2020**, *12*, 4975. [[CrossRef](#)]
13. Gámiz-Gordo, A.; Ferrer-Pérez-Blanco, I.; Reinoso-Gordo, J.F. The Pavilions at the Alhambra's Court of the Lions: Graphic Analysis of Muqarnas. *Sustainability* **2020**, *12*, 6556. [[CrossRef](#)]
14. Chen, S.; Yang, H.; Wangand, S.; Hu, Q. Surveying and Digital Restoration of Towering Architectural Heritage in Harsh Environments: A Case Study of the Millennium Ancient Watchtower in Tibet. *Sustainability* **2018**, *10*, 3138. [[CrossRef](#)]

15. Fadliand, F.; AlSaeed, M. Digitising Vanishing Architectural Heritage; The Design and Development of Qatar Historic Buildings Information Modeling [Q-HBIM] Platform. *Sustainability* **2019**, *11*, 2501. [CrossRef]
16. Alejandro, P.; Franco, C.; Rueda, A.; Plataand, M.D.; Franco, J.C. From the Point Cloud to BIM Methodology for the Ideal Reconstruction of a Lost Bastion of the Cáceres Wall. *Appl. Sci.* **2020**, *10*, 6609. [CrossRef]
17. Chudoba, P.; Przewłócki, J.; Samól, P.; Zabuski, L. Optimization of Stabilizing Systems in Protection of Cultural Heritage: The Case of the Historical Retaining Wall in the Wisłoujście Fortress. *Sustainability* **2020**, *12*, 8570. [CrossRef]
18. Reinoso-Gordo, J.F.; Rodríguez-Moreno, C.; Gómez-Blanco, A.J.; León-Robles, C. Cultural Heritage Conservation and Sustainability Based on Surveying and Modeling: The Case of the 14th Century Building Corral del Carbón (Granada, Spain). *Sustainability* **2018**, *10*, 1370. [CrossRef]
19. Angiolilli, M.; Gregori, A.; Vailati, M. Lime-Based Mortar Reinforced by Randomly Oriented Short Fibers for the Retrofitting of the Historical Masonry Structure. *Materials* **2020**, *13*, 3462. [CrossRef]
20. Frigione, M.; Lettieri, M.; Sarcinella, A.; Barroso de Aguiar, J.L. Applications of Sustainable Polymer-Based Phase Change Materials in Mortars Composed by Different Binders. *Materials* **2019**, *12*, 3502. [CrossRef] [PubMed]
21. Ramaglia, G.; Fabbrocino, F.; Lignola, G.P.; Prota, A. Unified Theory for Flexural Strengthening of Masonry with Composites. *Materials* **2019**, *12*, 680. [CrossRef]
22. Dong, K.; Sui, Z.; Jiang, J.; Zhou, X. Experimental Study on Seismic Behavior of Masonry Walls Strengthened by Reinforced Mortar Cross Strips. *Sustainability* **2019**, *11*, 4866. [CrossRef]
23. Wang, G.; Yang, C.; Pan, Y.; Zhu, F.; Jin, K.; Li, K.; Nanni, A. Shear Behaviors of RC Beams Externally Strengthened with Engineered Cementitious Composite Layers. *Materials* **2019**, *12*, 2163. [CrossRef] [PubMed]
24. Kociuba, W. Different Paths for Developing Terrestrial LiDAR Data for Comparative Analyses of Topographic Surface Changes. *Appl. Sci.* **2020**, *10*, 7409. [CrossRef]
25. Cano, P.; Álvarez, F.L.; Torres, J.C.; del Mar Villafranca, M. Use of 3D laser scanning to record the pre-intervention state of the Fuente de los Leones de La Alhambra. *Virtual Archaeol. Rev.* **2010**, *1*, 89–94. [CrossRef]
26. Huerta, S. *Arches, Vaults and Domes. Geometry and Equilibrium in the Traditional Calculation of Masonry Structures*; Instituto Juan de Herrera, Escuela Técnica Superior de Arquitectura Madrid: Madrid, Spain, 2004.
27. Wu, C. *Towards Linear-Time Incremental Structure From Motion, 3DV*; Institute of Electrical and Electronics Engineers: Seattle, WA, USA, 2013.
28. Wu, C. VisualSfM: A Visual Structure from Motion System. 2011. Available online: <http://ccwu.me/vsfm/5> (accessed on 27 June 2019).
29. Agisoft Metashape Professional. Agisoft Metashape Professional Version 1.5.1. Agisoft. 2019. Available online: <http://www.agisoft.com>. (accessed on 30 July 2020).
30. Leon, I.; Pérez, J.J.; Senderos, M. Advanced Techniques for Fast and Accurate Heritage Digitisation in Multiple Case Studies. *Sustainability* **2020**, *12*, 6068. [CrossRef]
31. Quagliarini, E.; Clini, P.; Ripanti, M. Fast, low cost and safe methodology for the assessment of the state of conservation of historical buildings from 3D laser scanning: The case study of Santa Maria in Portonovo (Italy). *J. Cult. Herit.* **2017**, *24*, 175–183. [CrossRef]
32. Pesci, A.; Bonali, E.; Galli, C.; Boschi, E. Laser scanning and digital imaging for the investigation of an ancient building: Palazzo d'Accursio study case (Bologna, Italy). *J. Cult. Herit.* **2012**, *13*, 215–220. [CrossRef]
33. Koutsoudis, A.; Vidmar, B.; Ioannakis, G.; Arnaoutoglou, F.; Pavlidis, G.; Chamzas, C. Multi-image 3D reconstruction data evaluation. *J. Cult. Herit.* **2014**, *15*, 73–79. [CrossRef]
34. Beltrami, C.D.; Cavezzali, F.; Chiabrando, A.; Iaccarino Idelson, G.; Patrucco, F. Rinaudo. 3D Digital And Physical Reconstruction Of A Collapsed Dome Using Sfm Techniques From Historical Images. *Int. Arch. Photogramm. Remote Sens. Spat. Inf. Sci.* **2019**, XLII-2/W11. Available online: <https://d-nb.info/1185647805/34> (accessed on 3 August 2021).
35. Loprencipe, G.; Moretti, L.; Ferraro, T.P.R. Railway Freight Transport and Logistics: Methods for Relief, Algorithms for Verification and Proposals for the Adjustment of Tunnel Inner Surfaces. *Sustainability* **2018**, *10*, 3145. [CrossRef]
36. Ferrer-Pérez-Blanco, I.; Gámiz-Gordoand, A.; Reinoso-Gordo, J.F. New Drawings of the Alhambra: Deformations of Muqarnas in the Pendentives of the Sala de la Barca. *Sustainability* **2019**, *11*, 316. [CrossRef]
37. Blanco, S.; Carrión, B.; Lerma, J.L. *Heritage Documentation through Photogrammetric and Laser Scanning Solutions, and Their Orientation to the Generation of Virtual Environments. La Ciencia y el Arte V. Experimental Sciences and Heritage Conservation*; Subdirección General de Documentación y Publicaciones: Madrid, Spain, 2015; pp. 56–69.
38. Ministry of Housing. *Basic Document: Structural Safety: Masonry. CTE DB SE-F*; Ministry of Housing: Madrid, Spain, 2006.
39. Torroja Miret, E. *Razón y ser de los Tipos Estructurales*; Instituto E. T. de la Construcción y del Cemento: Madrid, Spain, 2016.
40. Beben, D.; Ukleja, J.; Maleska, T.; Anigacz, W. Study on the Restoration of a Masonry Arch Viaduct: Numerical Analysis and Lab Tests. *Materials* **2020**, *13*, 1846. [CrossRef] [PubMed]
41. De la Plata, A.R.M.; Cruz Franco, P.A. A Simulation Study to Calculate a Structure Conceived by Eugène Viollet-le-Duc in 1850 with Finite Element Analysis. *Materials* **2019**, *12*, 2576. [CrossRef]
42. Pomares, J.C.; González, A.; Saura, P. Simple and resistant construction built with concrete voussoirs for developing countries. *J. Constr. Eng. Manag.* **2018**, *144*, 04018076. [CrossRef]

43. Santiago, H.F. *Diseño Estructural de Arcos, Bóvedas y Cúpulas en España c.a. 1500–c.a. 1800*. Ph.D. Thesis, Escuela Técnica Superior Arquitectura de Madrid (ETSAM), Madrid, Spain, 1990.
44. Delbecq, J.M. *Analyse de la Stabilité des Ponts en Maçonnerie par la Théorie du Calcul à la Rupture*. Ph.D. Thesis, Ecole Nationale des Ponts et Chaussées, Ecole des Ponts ParisTech Paris, Paris, France, 1983.
45. Šekularac, N.; Ristić, N.D.; Mijović, D.; Cvetković, V.; Ivanović-Šekularac, S.B.J. The Use of Natural Stone as an Authentic Building Material for the Restoration of Historic Buildings in Order to Test Sustainable Refurbishment: Case Study. *Sustainability* **2019**, *11*, 4009. [[CrossRef](#)]
46. Mazzola, E.; Mora, T.D.; Peron, F.; Romagnoni, P. An Integrated Energy and Environmental Audit Process for Historic Buildings. *Energies* **2019**, *12*, 3940. [[CrossRef](#)]
47. Corradi, M.; Borri, A.; Castori, G.; Coventry, K. Experimental Analysis of Dynamic Effects of FRP Reinforced Masonry Vaults. *Materials* **2015**, *8*, 8059–8071. [[CrossRef](#)] [[PubMed](#)]